Ecosystems
https://doi.org/10.1007/s10021-023-00877-7

Compensatory Mechanisms Absorb Regional Carbon Losses Within a Rapidly Shifting Coastal Mosaic

Alexander J. Smith,[1,2]* Karen McGlathery,[3] Yaping Chen,[1] Carolyn J. Ewers Lewis,[3] Scott C. Doney,[3] Keryn Gedan,[4] Carly K. LaRoche,[3] Peter Berg,[3] Michael L. Pace,[3] Julie C. Zinnert,[5] and Matthew L. Kirwan[1]

[1]*Department of Physical Sciences, Virginia Institute of Marine Science, College of William and Mary, Gloucester Point, Virginia, USA;* [2]*Smithsonian Environmental Research Center, Edgewater, Maryland, USA;* [3]*Department of Natural Sciences Flagler College, Saint Augustine, Florida, USA;* [4]*Department of Biological Sciences, George Washington University, Washington, District of Columbia, USA;* [5]*Department of Biology, Virginia Commonwealth University, Richmond, Virginia, USA*

Abstract

Coastal landscapes are naturally shifting mosaics of distinct ecosystems that are rapidly migrating with sea-level rise. Previous work illustrates that transitions among individual ecosystems have disproportionate impacts on the global carbon cycle, but this cannot address nonlinear interactions between multiple ecosystems that potentially cascade across the coastal landscape. Here, we synthesize carbon stocks, accumulation rates, and regional land cover data over 36 years (1984 and 2020) for a variety of ecosystems across a large portion of the rapidly transgressing mid-Atlantic coast. The coastal landscape of the Virginia Eastern Shore consists of temperate forest, salt marsh, seagrass beds, barrier islands, and coastal lagoons. We found that rapid losses and gains within individual ecosystems largely offset each other, which resulted in relatively stable areas for the different ecosystems, and a 4% (196.9 Gg C) reduction in regional carbon storage. However, new metrics of carbon replacement times indicated that it would take only ~ 7 years of carbon accumulation in surviving ecosystems to compensate this loss. Our findings reveal unique compensatory mechanisms at the scale of entire landscapes that quickly absorb losses and facilitate increased regional carbon storage in the face of historical and contemporary sea-level rise. However, the strength of these compensatory mechanisms may diminish as climate change exacerbates the magnitude of carbon losses.

Key words: coastal carbon dynamics; ecosystem transition; ghost forest; blue carbon; landscape-scale carbon storage; compensatory mechanisms.

Introduction

The ability of ecosystems, communities, and populations to absorb environmental change and reorganize so as to retain structure and function has been a hallmark of resilience and compensation research (Folke and others 2004; Ghedini and others 2015). Compensatory dynamics, occurring

Received 3 March 2023; accepted 10 August 2023

Supplementary Information: The online version contains supplementary material available at https://doi.org/10.1007/s10021-023-00877-7.

Author Contributions: All authors conceived and designed the study at various LTER VCR meetings. AJS, YC, and CKL performed research and analyzed data. Data was provided by KM, SCD, KG, PB, MLP, and JCZ. AJS wrote the paper and all co-authors assisted in editing and revising the manuscript.

*Corresponding author; e-mail: SmithAJ1@si.edu

Published online: 15 September 2023

when an environmental change stimulates a counteracting response that reestablishes equilibrium, are expected to be an important stabilizing mechanism through which communities respond to environmental change (Gonzalez and Loreau 2009; Ghedini and others 2015). While compensatory dynamics have a long history in community and population ecology (Gonzalez and Loreau 2009), this framework can also provide insights into the mechanisms that potentially stabilize ecosystem extent and function, a growing concern in the face of accelerating changes in global climate (MacArthur and others 1972; Houlahan and others 2007; Loreau and de Mazancourt 2013; Ghedini and others 2015). This presents the opportunity to expand the traditional application of compensatory mechanisms to explore the novel concepts of spatial and functional compensation, processes necessary for stabilizing entire ecosystems and landscapes in a rapidly changing climate.

Spatial compensation, an expansion of compensation theory, occurs where losses and gains of an individual ecosystem in different locations offset each other, thereby maintaining ecosystem area within the broader region. The preservation of area in migrating ecotones, such as the sea-level driven upland transgression of marshes, poleward expansion of subarctic forests, and upslope migration of alpine ecoclines, are all examples of the principles of spatial compensation across a variety of environmental settings (Maher and others 2005; Gamache and Payette 2005; Schieder and others 2018). Functional compensation is independent of spatial compensation and is defined by the preservation of an ecosystem function, despite reductions in process rates within ecosystem subunits (that is, subregions or habitats) due to environmental change (Lawton and Brown 1993). These compensations may be realized as heterogenous responses to environmental changes across the landscape, such as when salt marsh interiors accumulate increased carbon under elevated rates of sea-level rise despite losing carbon through sea-level mediated edge erosion (Herbert and others 2021). Climate change affects both ecosystem extent and function, often simultaneously, which allows spatial and functional compensation to be used as theoretical frameworks to examine the legacy effect of climate change on landscape dynamics.

Climate change is forcing transitions between coastal ecosystems at an increasing rate that can lead to large-scale ecosystem degradation and loss (Bernhardt and Leslie 2013; Doney and others 2012). For example, accelerating rates of sea-level rise are leading to increased marsh erosion and degradation as well as the burial of back-barrier marshes beneath transgressing barrier islands (Fitzgerald and Hughes 2019; Fagherazzi and others 2020; Theuerkauf and Rodriguez 2015). Co-occurring climate drivers, such as increasing temperatures and elevated atmospheric CO_2 concentrations, further threaten coastal ecosystems by exceeding the biological limits of foundational species (Smith and others 2022; Noyce and others 2022). Anthropogenic effects, such as alterations to sediment budgets, eutrophication, and urbanization, can further accelerate habitat degradation (Hartig and others 2002; Kirwan and Megonigal 2013). There is widespread evidence that direct and indirect anthropogenic influences have changed the distribution, extent, and function of habitats that comprise the coastal landscape mosaic (for example, Ewers Lewis and others 2019), but these simultaneous changes to ecosystem structure and function have unclear effects on regional functions, including carbon storage. Moreover, impacts have rarely been examined at the scale of the landscape, rather than that of an individual ecosystem, where inter-ecosystem spatial and functional compensatory mechanisms can emerge.

As the coastal landscape changes, carbon rich ecosystems, such as seagrass meadows and salt marshes, are often replaced with unvegetated sediments that should reduce regional carbon storage in the absence of compensatory mechanisms and other landscape-scale interactions between ecosystems (Mcleod and others 2011; Trevathan-Tackett and others 2018; Garrard and Beaumont 2014; Aoki and others 2020). Studies have attempted to look at the impact of degraded blue carbon habitat (that is, marshes, seagrass meadows, mangroves) on regional and global carbon storage (Siikamäki and others 2013; Macreadie and others 2017; Ewers Lewis and others 2019), but many of these studies neglect to consider functional or spatial gains in distal areas of the coastal landscape. For example, while marshes drowning under sea-level rise reduce marsh area and release stored carbon, increasing sea-level rise drives simultaneous increases in carbon accumulation in the marsh interior (Herbert and others 2021; Guimond and others 2020). Furthermore, sea-level rise creates new marsh at the upland boundary additionally compensating for the spatial and functional losses at the seaward edge (Smith and Kirwan 2021; Schieder and others 2018). At the same time, there is substantial amount of carbon lost from dying tree biomass during the upland transgression of marshes into forested land (Smith and Kirwan 2021; Smart and others 2020). Therefore, solely exam-

ining carbon dynamics in specific carbon-rich ecosystems is unsatisfactory in understanding how coastal carbon dynamics are changing regionally. While similar studies that estimate regional carbon storage may concentrate on changes in specific boundaries (He and others 2016; Fryer and Williams 2021), the nonlinear, non-uniform, and co-occurring nature of ecosystem transitions within the coastal zone requires the examination of the entire coastal landscape mosaic inclusive of the many terrestrial, intertidal, benthic, and epipelagic habitats that comprise it.

Here, we synthesize nearly 40 years of carbon and land cover data across a rapidly transgressing coastal landscape to show that rapid spatial and functional compensatory mechanisms maintain both ecosystem extents and regional carbon storage despite sometimes substantial ecosystem losses. We used land cover data from Landsat images between 1984 and 2020 to quantify increases, decreases, and net changes in ecosystem extent. Multiplying ecosystem extents by area-specific carbon stocks produced landscape-scale carbon stocks for both 1984 and 2020. Using the change in regional carbon stocks and ecosystem-scale carbon burial rates, we then calculated the 'time to replacement' at the regional scale, which is an estimate of the time required for all of the carbon accumulating environments in the landscape to replace the carbon that was lost between 1984 and 2020. Our analysis shows that compensatory mechanisms largely maintain the spatial extent of the most dynamic ecosystems (that is, barrier islands and salt marshes), but that declines in forest and marsh area led to a small decrease in landscape-scale carbon storage. We calculate that surviving ecosystems compensate for the decadal loss of carbon storage rapidly, suggesting that compensatory mechanisms quickly restore functionality at the landscape scale despite accelerating climate stressors.

Methods

Study Area

We quantified land cover changes, carbon stocks, and carbon accumulation rates for a variety of ecosystems along the Virginia Atlantic coast, a known hotspot for sea-level rise and ecosystem transgression in the United States (Chen and Kirwan 2022a; Mariotti and Hein 2022). The Virginia Coast Reserve (VCR) was established in 1970 by the Nature Conservancy and is the site of the VCR Long-Term Ecological Research (LTER) project. The coastal landscape includes 14 undeveloped barrier and marsh islands, intertidal marshes, tidal flats, bays, and lagoons that make up the eastern side of the Delmarva Peninsula along the Virginia Atlantic Coast (Figure 1a, b). With a spatial extent > 14,000 ha, this is the largest undeveloped barrier system along the U.S. Atlantic Coast and, consequently, provides a unique opportunity to study landscape transformations in the absence of direct human alteration (Hayden and others 1991). Our study area is bounded on the east by nine barrier islands, which range from 3–12 km long and 0.1–1.0 km wide and are located 2.0–13.5 km offshore (Deaton and others 2017). The back-barrier landscape is a heterogenous mosaic of salt marshes, tidal flats, and subtidal seagrass meadows surrounded by open water with an average depth of 1 m and a tidal range of $\sim$ 1.2 m (Figure 1a, b; Safak and others 2015; McLoughlin and others 2015). This region experiences some of the highest rates of relative sea-level rise along the U.S. Atlantic Coast (5.4 ± 0.7 mm y^{-1} from 1978 to 2019) (Sallenger and others 2012; Flester and Blum 2020). Consequently, relatively rapid rates of marsh migration into coastal forests (up to 4.0 m y^{-1} lateral migration) and barrier island retreat (up to 1.5 m y^{-1}) are quickly reorganizing the coastal landscape (Figure 1c–e; Deaton and others 2017; Fenster and others 2016; Flester and Blum 2020). Additionally, the study area includes the largest recovery of an eelgrass ecosystem to date (McGlathery and others 2012; Orth and McGlathery 2012; Orth and others 2020). Not only do long-term data collected show that the VCR is one of the most dynamic coastal barrier island landscape on the U.S. Atlantic seaboard (May and others 1983; Morton 2008; Fenster and others 2016), but the extensive catalog of long-term monitoring data available through past research at the VCR makes this one of the most studied undeveloped coastal barrier systems in the U.S. (SI Table 1).

Mapping Land Cover Change

To quantify climate-driven land cover change in a shifting coastal mosaic, we gathered Landsat satellite imagery covering the study area between 1984 and 2020 with cloud cover < 60% from the USGS EarthExplorer collected by Landsat-5 TM and Landsat-8 OLI. All images were processed using the ancillary Quality Assessment dataset to mask out pixels associated with clouds, cloud shadows, and ice. We restricted our land cover analysis to the portion of the landscape between sea-level and elevations of 2 m above sea-level (NAVD88) according to the high-resolution topobathymetric

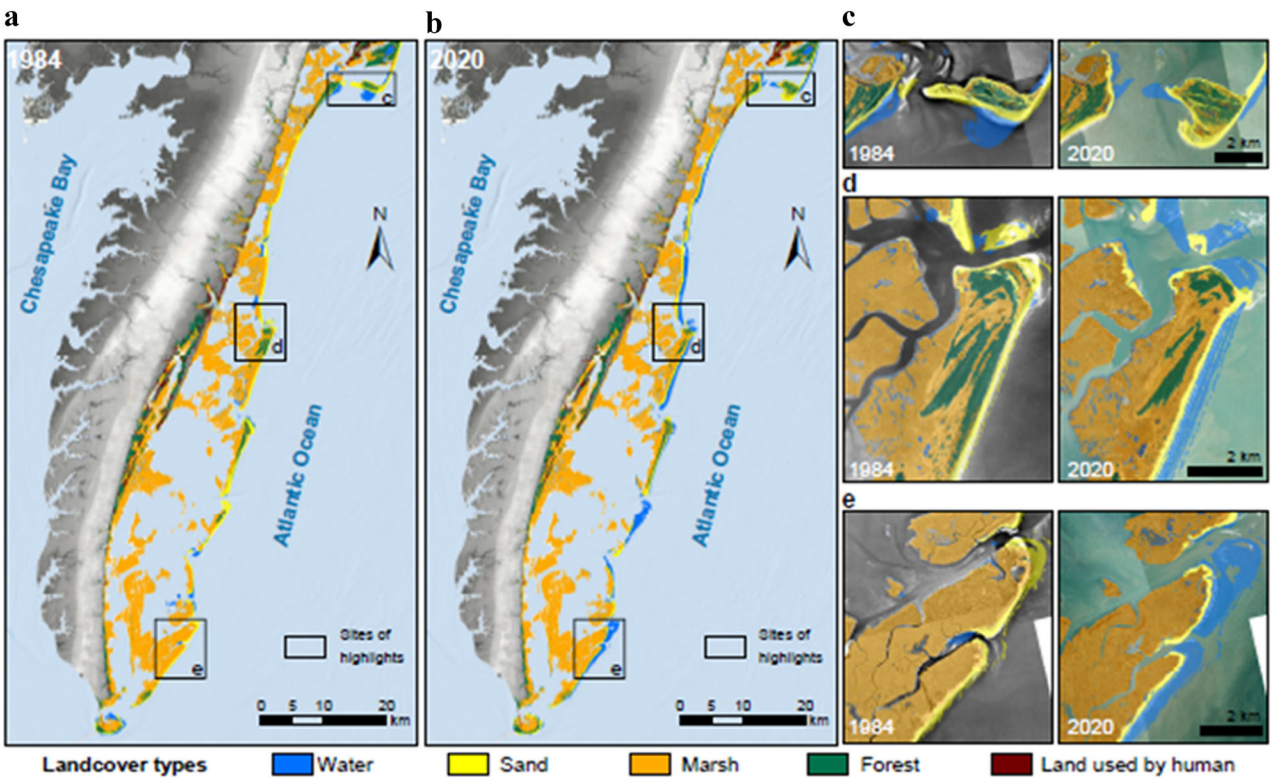

Figure 1. Land cover maps of the study area, the Virginia Coastal Reserve, on the Delmarva Peninsula in 1984 (**a**) and 2020 (**b**) (base map in **a** and **b** ArcGIS v10.7). Black boxes in **a** and **b** indicate locations of representative ecosystem transitions common throughout the Virginia Coastal Reserve: barrier island expansion (**c**), barrier island erosion and coastal forest reduction (**d**), and barrier island retreat over back barrier marshes (**e**). The land cover maps in panels **c**, **d** were plotted on top of high-resolution aerial images acquired around 1984 from the U.S. Bureau of Land Management (displayed in black and white) and 2020 from the National Agriculture Imagery Program (displayed in color) with respective land cover classifications superimposed atop the imagery.

digital elevation model of the Eastern Shore, which has a horizontal resolution of 1 m and a vertical resolution of 1 cm (Faunce and Rapp 2020). This elevation range excluded deep, permanent waters within inlet channels and seaward of barrier islands while including the majority of coastal forests influenced by sea-level rise in the region (Molino and others 2021; Chen and Kirwan 2022a). Imagery was further clipped to our region of interest (that is, the VCR-LTER) before mapping with random forest classifier in R (v. 4.1.1, packages of '*caret*' and '*randomForest*'). Specifically, we classified the area of interest into five land cover types following the phenology-based algorithm described in detail by Chen and Kirwan (2022b): Water, Sand, Marsh, Forest, and lands used by humans (abbreviated in this manuscript to Human). The resulting land cover maps in 1984 and 2020 were thoroughly validated with high-resolution imagery (≤ 1 m) acquired from the U.S. Bureau of Land Management and National Agriculture Imagery Program across the study region that suggest an overall classification accuracy of 94–96% within the VCR-LTER (SI Table 2).

Seagrass extent was quantified separately using seagrass extent data in 2017 collected by the SAV Monitoring and Restoration group at the Virginia Institute of Marine Science (vims.edu/research/units/programs/sav/reports/index.php). In 1984, the seagrass extent was assumed to be zero due to extirpation within the VCR (Orth and McGlathery 2012; Orth and others 2020). The spatial extent of barrier islands, not an explicit class in this paper's land cover classification scheme, was calculated manually by delineating island extents from high-resolution (≤ 1 m) aerial photographs acquired around 1984 (Aerial Photo Single Frames, the U.S. Bureau of Land Management and USGS Earth Explorer) and 2020 (the National Agriculture Imagery Program, NAIP).Using the resulting maps, we estimated the spatial extent of each of the seven land cover types in 1984 and 2020, and quantified the areal change between 1984 and 2020 for each land cover across the study region (Table 1). We

Table 1. Cross Tabulation Matrix for Land Cover Change from 1984 to 2020 Showing the Extent of Land Cover Category Persistence and Change (km^2) During the Time Interval

		Landcover in 1984 (km^2)						
		Water	Forest	Marsh	Human	Sand	Seagrass*	**Gains**
Landcover in 2020 (km^2)	Water	14.7	1.68	14.3	0.09	22.3	0	38.3
	Forest	0.66	43.9	0.0	4.33	4.33	0	7.16
	Marsh	3.35	6.58	292	0.70	2.52	0	13.1
	Human	0.01	1.14	0.10	16.4	0.05	0	1.29
	Sand	9.07	0.76	11.4	0.04	7.82	0	20.2
	Seagrass*	29.3	0	0	0	0	0	29.3
	Losses	12.2	10.1	25.8	5.12	27.0	0	
	Net Change	26.2	-3.00	-12.6	-3.84	-6.78	29.3	

**Indicates that the change in seagrass extent was quantified using the VIMS seagrass database.*

then conducted pixel-wise analysis using the differenced land cover map between 1984 and 2020 in ArcGIS (v10.7) to locate areas undergoing land cover transition and to record the land cover information associated with these transitions (Table 1).

Estimates of Regional Carbon Storage

Regional carbon storage was estimated by synthesizing carbon stocks reported in previous work, with an emphasis on datasets specific to the Virginia Coastal Reserve ranging from 1990 to 2021 (SI Table 1). Our study focused on four vegetated systems (forests, marshes, seagrasses, and barrier islands) known to contribute significant amounts of carbon to regional and global carbon storage (Mcleod and others 2011). Unvegetated tidal flats and bare underwater sediments were excluded from this analysis because of limited data on spatial extents and limited influence on coastal carbon storage, respectively. Our reported carbon stocks for these systems represent the carbon stored in soils and living aboveground and belowground biomass. A majority of the datasets reported both above- and belowground carbon stocks, except for barrier islands where a species-specific root-to-shoot ratio was used to approximate belowground biomass. Biomass was then converted to carbon using respective above- or belowground species-specific conversion factors for marsh grass and seagrass vegetation. When a conversion factor was unavailable or the species not listed (for example, barrier island vegetation, some marsh and forest species), biomass was converted to carbon using a standard 50% conversion. Soil carbon measurements for seagrasses and some marsh sites were quantified directly while soil carbon in barrier islands, forests, and some marsh sites were inferred from a general or site-specific percent organic matter (%OM) to carbon relationship. To similarly scale all ecosystems to a spatially explicit carbon density (g C m^{-2}), soil %OM and carbon stock measurements deeper than 1 m, such as those in salt marshes, were excluded. For ecosystems with organic matter depths shallower than 1 m, soil beneath the deepest measurement was assumed to have no carbon (SI Table 1). Once the carbon stock was determined for a specific ecosystem type, it was multiplied by the spatial extent of the corresponding ecosystem in both 1984 and 2020 to estimate the regional carbon stock of each vegetated ecosystem. Carbon accumulation rates were calculated from datasets that used cesium-137 (^{137}Cs) in salt marshes and barrier islands, and lead-210 (^{210}Pb) in seagrasses. In salt marshes, the average soil carbon accumulation rate was 78.4 g C m^{-2} y^{-1}, in seagrass meadows the average was 40.0 g C m^{-2} y^{-1}, and in barrier islands the average was 21.9 g C m^{-2} y^{-1}.

In addition to these vegetated systems, we considered carbon stored in the water column as dissolved inorganic carbon (DIC). DIC in the water column was approximated using the CO2SYS MATLAB 1.1 package and total alkalinity (TA), pCO_2, temperature, and salinity data (Ewers Lewis and others 2019; Van Heuven and others 2011; Orr and others 2015, 2018). Hourly water column pCO_2, temperature, and salinity data were collected in April and June in South Bay in the VCR (Berger and others 2020). TA was calculated using Cai and others' (2010) linear regression, TA = 670.6 + 46.6

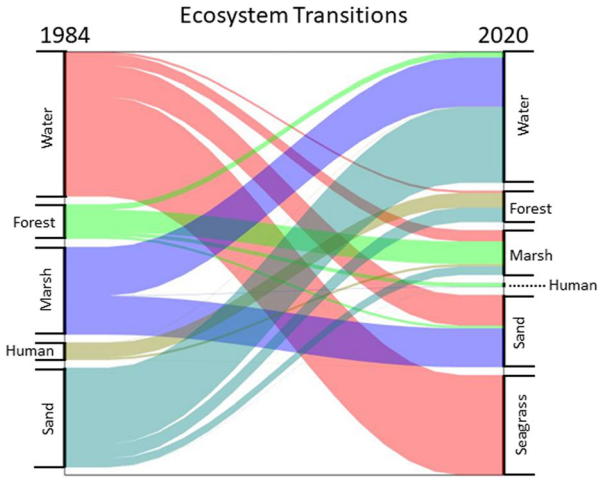

Figure 2. Sankey diagram showing ecosystem transition between two time intervals, 1984 and 2020, within the VCR coastal network. Stable pixels—pixels within the landscape that did not change land cover—are excluded from this visualization for clarity as stable pixels comprise ~ 80% of the coastal landscape.

S ± 12.3 μmol kg^{-1}, for the Mid-Atlantic Bight, where S is salinity. The average VCR volume, 979.7 ± 126 million cubic meters (Mm^3), was calculated by multiplying area by average depth in 14 bays and summing the resulting volumes (Safak and others 2015). The average water-column DIC concentration was multiplied by the seawater mass of the VCR lagoon system, 1 Pg, which had been calculated from average seawater density and the average volume (Safak and others 2015).

Calculating Time to Replacement

Following Smith and Kirwan (2021), the ''time to replacement'' metric, t_r, can be used to estimate the time required for ecosystem carbon accumulation rates, CAR, to replace losses in carbon stocks, C_L (that is, $t_r = C_L/CAR$). In past applications of the metric, it has been used to look at the carbon lost and replaced over time at a fixed location (that is, during the transition from forest to marsh at a given point in space). Below, we extend the application of time to replacement to the ecosystem and landscape scales to estimate the amount of time it takes entire carbon accumulating ecosystems within the coastal landscape of the VCR to replace the carbon that was lost from 1984 to 2020.

A meter-scale time to replacement, t_r^{meter} (y), can be defined as the amount of time that the carbon stock from the loss of a 1 m^2 of ecosystem x, C_x (g C m^{-2}), could be replaced by a spatially explicit carbon accumulation rate, CAR_y (g C m^{-2} y^{-1}), of ecosystem y where the areas of carbon loss and carbon accumulation are equivalent:

$$t_r^{meter}(x,y) = \frac{C_x}{CAR_y} \quad (1)$$

where x and y can be the same or different ecosystems (Smith and Kirwan 2021). We extend this equation to consider the regional effect of carbon loss from a reduced ecosystem area on t_r as an ecosystem-scale time to replacement, t_r^{eco} (y), as be defined as:

$$t_r^{eco}(x,y) = \frac{C_x \Delta A_x}{CAR_y A_y} \quad (2)$$

where ΔA_x is the observed change in ecosystem area within a timeframe (1984 to 2020 in this study) for ecosystem x (m^2), and A_y is the time averaged area of ecosystem y (m^2). This equation can be further modified to consider the sum of all the carbon accumulating ecosystems, called the landscape-scale time to replacement, t_r^{land}:

$$t_r^{land}(x,\Sigma) = \frac{C_x \Delta A_x}{\sum_i CAR_i A_i} \quad (3)$$

where $\sum_i CAR_i A_i$ is the total carbon accumulation rate of all ecosystems within the coastal landscape. Finally, to encapsulate multiple simultaneous changes in ecosystem carbon storage within the landscape, the modified form of a landscape time to replacement can be expressed as:

$$t_r = \frac{C_{land}}{\sum_i CAR_i A_i} \quad (4)$$

where C_{land} (g) is the net carbon lost at the landscape scale across all ecosystems, $\sum(CAR_i * A_i)$ is the carbon accumulation rate (CAR_i, g C m^{-2} y^{-1}) of all of the ecosystems (i) within the coastal landscape multiplied by the respective ecosystem area (A_i, m^2).

Results

Land Cover Changes and Carbon Dynamics

The land cover change analyses revealed that over 80% of the study area, the Virginia Coast Reserve (VCR), remained the same class in 1984 and 2020 (Figure 1a, b, Table 1). The stable portion of the landscape with respect to total area was comprised mostly of temperate salt marsh rather than the more dynamic landscape features, such as barrier islands and seagrass. The VCR coastal landscape was dominated by marsh (70% and 67%), forest

Table 2. The Spatial Extent (km^2) of Land Cover Classes and Ecosystem Carbon Storage (Gg C) in 1984 and 2020 and the Change Between These Dates

Land cover classification	1984 (km^2)	2020 (km^2)	Percent change (%)	1984 (Gg C)	2020 (Gg C)	Carbon storage change (Gg C)
Water	26.7	53.0	98	23	23	0
Marsh	318.0	305.4	− 4	3711	3564	− 147
Human	21.5	17.7	− 18	N/a	N/a	N/a
Forest	54.1	51.1	− 5	754	712	− 41
Seagrass	0*	29.3	> 100	0*	8.66	+ 8.66
Sand/Barrier Islands	34.8	28.0	− 20	75.9	59.4	− 16.5
			Total:	4563.9	4366.9	− 196.9

Indicates that there were no detectable seagrass meadows within the study area in 1984. N/A indicates that no carbon stock data was collected for agricultural or urban areas.

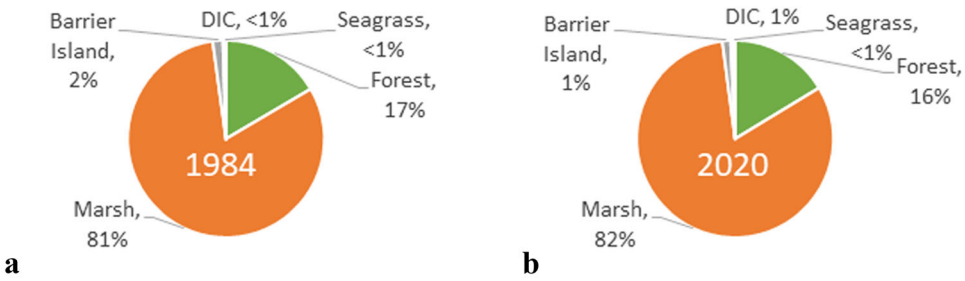

Figure 3. Pie charts indicating the contribution of the coastal ecosystem's carbon stocks (marshes, coastal forests, barrier islands, seagrass, and DIC in the water column) to the regional carbon budget in 1984 (**a**) and 2020 (**b**).

(12% and 11%), and open-water (6% and 12%) in both years (1984 and 2020, respectively, Table 2). The proportion of sand land cover class remained relatively stable at the landscape scale (7%), and human areas remained < 5% of the landscape in 1984 and 2020 (Table 2). The areas of individual ecosystems all decreased except for seagrass and water, which nearly doubled from 26.7 to 53.0 km^2. Forest area decreased by 5.5% (54.0 to 51.0 km^2) and marsh area decreased by 4.0% (318 to 305 km^2). Both sand and human area decreased by ~ 18% (Table 2). The largest land cover change observed was seagrass, which increased from ~ 0 to 29.3 km^2 (increased from ~ 0% to 6.4% of landscape cover) in response to widespread restoration efforts beginning in 2000 that returned seagrass populations that had been extirpated from the coastal lagoons following marine disease and hurricane disturbance in the 1930s (Orth and McGlathery 2012). Conversion of water and marsh to sand were the dominant contributors to sand creation (39.9% and 56.3% of sand creation, respectively) and can be best explained by barrier island rollover and migration (Figures 1e, 2). The dominant driver of forest loss was marsh migration (64.8%) followed by the elimination of forested areas on barrier islands (23.9%) (Figure 2). Despite large increases in marsh area near adjacent upland edges (6.6 km^2), losses of marsh at the seaward side (14.3 km^2) offset these gains leading to a 4% net loss of marsh area (Table 2). This approach does not account for any temporary transitions between classification years.

Area-specific carbon storage ranged from 13.9 ± 4.6 (SE) kg C m^{-2} in marshes to 0.30 ± 0.8 kg C m^{-2} in seagrass within the VCR (SI Table 1). A landscape-scale analysis indicated that a majority of carbon within the VCR region was stored in the salt marsh (81% in 1984 and 82% in 2020) (Figure 3). Forest carbon was the second largest contributor to regional carbon storage (17% and 16%) while carbon in the water column, seagrasses, and barrier islands all contributed < 3% to the regional carbon storage (Figure 3). Carbon stored in anthropogenic dominated environments (agricultural fields, residential housing, and urbanized areas) were not included in regional carbon estimates, but are expected to contribute negligibly to regional carbon storage given the limited extent within the studied coastal domain (Figure 1a, b). Regional

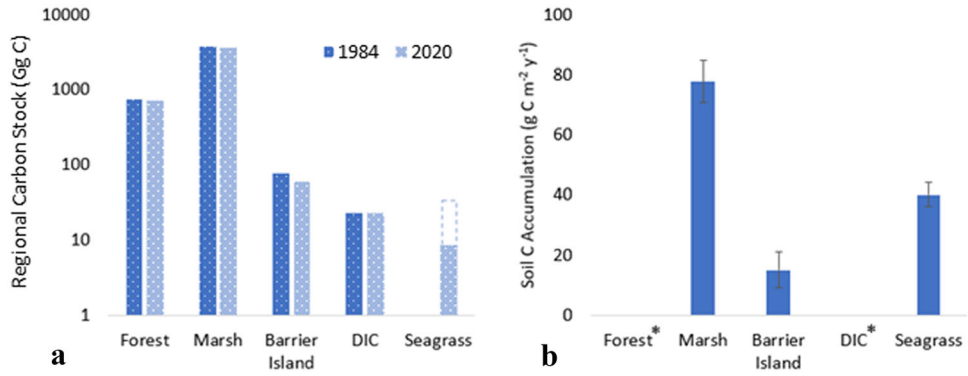

Figure 4. (**a**) The carbon stocks (Gg C) of individual coastal ecosystems in 1984 and 2020. Note the data is presented on a log scale. The dashed box above the seagrass stock represents the potential increase in seagrass carbon stock if soils were able to accumulate carbon to comparable depths (that is, 40 cm) (**b**) Soil carbon accumulation rates (g C m^{-2} y^{-1}) of coastal ecosystems (mean ± standard error). *While we assume negligible rates for these ecosystems, we recognize that there may be some depositional accumulation of carbon.

carbon storage decreased by 4%, from 4563.9 in 1984 to 4366.9 Gg C in 2020 (Table 2; Figure 4). This landscape-scale loss of 196.9 Gg C occurred despite large increases in carbon storage in seagrass, which recolonized in the VCR during the study period. The dominant driver of this loss was the reduction of marsh and forested land, which together accounted for over 95% of the carbon lost between 1984 and 2020 (Figures 3; 4). These changes in regional carbon storage were driven by changes in spatial extent as our estimates do not consider changing environmental factors that could impact the carbon density of an ecosystem, such as temperature, precipitation, atmospheric CO_2, age, or sea-level (Smith and Kirwan 2021).

Landscape-scale Time to Replacement

A meter-scale time to replacement (Eq. 1) can be defined as the amount of time that the carbon stock from the loss of a square meter of an ecosystem could be replaced by a spatially explicit carbon accumulation rate of a different ecosystem where the areas of carbon loss and carbon accumulation are equivalent. For example, the large carbon stock in 1 m^2 of forest, C_{forest} = 13,295 g C m^{-2}, would take 169.6 years to be replaced by carbon accumulation rates in 1 m^2 of marsh, CAR_{marsh} = 78.4 g C m^{-2} y^{-1} (Eq. 1; SI Table 1). However, our land cover change analysis indicates that within our study area, far greater than 1 m^2 of forest was lost (Table 1). Additionally, we should consider the entire spatial extent of the marshes within our study area that were simultaneously accumulating carbon (Eq. 2). Therefore, when we consider the cumulative area of marshes within our study area and the amount of forest lost between 1984 and 2020, the ecosystem-scale time to replacement (Eq. 2) is 1.7 years—far less than the previous meter-scale time to replacement. This is driven by the small area of lost forest (3.0 km^2) relative to the extant marsh (305 km^2). When considering the sum of all carbon accumulating ecosystems (Eq. 3), the landscape time to replacement for the loss of forest carbon is reduced to 1.6 years, which is relatively similar to the previous calculation due to the dominance of salt marshes within the coastal environment. Finally, when we integrate the cumulative carbon lost from reductions in all ecosystems' extents (Eq. 4), we find that it takes approximately 7.42 ± 0.75 years to replace the carbon that was lost (that is, 196.9 Gg C) from 1984–2020 (36 years).

Discussion

Coastal ecosystems are rapidly migrating in response to sea-level rise, leading to a fundamental reorganization of the coastal landscape (Doody 2013; Deaton and others 2017; Fitzgerald and Hughes 2019; Kirwan and Gedan 2019). Despite visible differences in land cover (Figure 1c–e), the total spatial extent for individual ecosystems changed very little between 1984 and 2020 (Figure 1a, b, Table 1). We attribute this spatial compensation to widespread but equivalent gains or losses in individual ecosystems (Tables 1, 2). This indicates that despite significant changes in the location of individual ecosystems, spatial compensation largely maintains the total extent of each ecosystem (Tables 1, 2), which is consistent with observations from a number of other coastal and terrestrial ecosystems (Turner 2010; Smith and

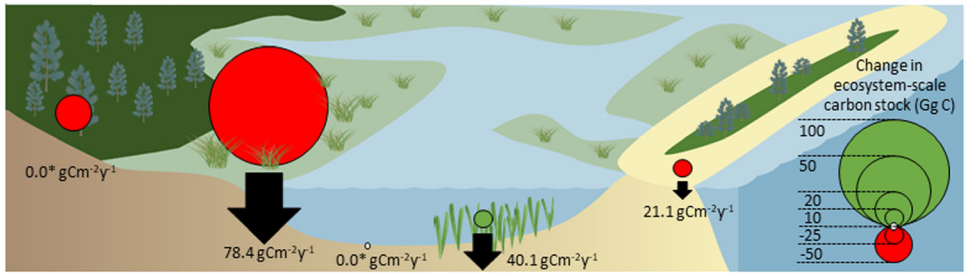

Figure 5. Changes in ecosystem carbon stocks in the coastal landscape from 1984 to 2020: forests (dark green), marshes (light green), DIC (blue; note no change in carbon stock), seagrass (benthic grass icons), and barrier islands (beige surrounding dark green). The size of the circle superimposed on each ecosystem indicates the magnitude of carbon stock change (Gg C) from 1984 to 2020 while the color of the circle portrays positive (green) or negative (red) changes. Arrows and the accompanying numbers represent the soil carbon accumulation rates measured in each of these ecosystems and follow the same size scale as the circles. *While we assume negligible rates of soil carbon accumulation by the forest and DIC pools, we recognize that there may be some depositional accumulation of carbon.

Goetz 2021) and for the VCR from 1972–2001 (McGlathery and others 2013). For example, barrier islands tend to migrate landward while maintaining relative area (Deaton and others 2017), and marsh erosion is compensated by marsh migration regionally (Schieder and others 2018). While spatial compensation can be observed within at least some individual ecosystems of the VCR (Burns and others 2021; Flester and Blum 2020), this represents one of the first studies to examine spatial compensation across multiple ecosystems at the landscape scale.

The shifting mosaic steady-state concept suggests that the overall ecosystem composition is maintained in a landscape despite shifts in ecosystem location (Bormann and Likens 2012; Forman 2014). Although our observations of spatial compensation within salt marshes are consistent with the shifting mosaic steady-state theory, some ecosystems did not maintain consistent spatial extents. We observed significant decreases in forested land and sand and increases in seagrass that were not compensated elsewhere in the landscape (Table 2). Marsh migration into retreating forests was not compensated for by migration of forests into adjacent uplands due to topography and anthropogenic land uses, resulting in coastal squeeze of forested ecosystems (Figure 2) (Torio and Chmura 2013; Pontee 2013). Similarly, the net decrease of sand within the landscape is driven by erosion and colonization of barrier island overwash fans that was not compensated by back-barrier spit elongation (Figure 2). However, in similar studies, changes in barrier island extent observed over two different time frames (from 1984 to 2011 and from 1984 to 2016) were drastically different, a 29% reduction and a 11% increase in spatial extent respectively, which emphasizes that temporal scale and the timing of measurements can dictate apparent spatial patterns (Zinnert and others 2016, 2019).

The lack of spatial compensation in forested land compounds with reduced blue carbon storage to increase the observed reduction in regional carbon storage (Figures 4, 5, Table 2). Area-specific carbon storage ranges within the VCR from 11.7 kg C m^{-2} in marshes to 0.30 kg C m^{-2} in seagrass (SI Table 1). Marsh carbon storage, 11.7 kg C m^{-2}, was found to be smaller than the average carbon storage in marshes of the conterminous United States (27.0–28.0 kg C m^{-2}), Europe (26.1 kg C m^{-2}), and Southeastern Australia (25.3 kg C m^{-2}), but within the range of measured soil carbon stocks (Holmquist and others 2018; Nahlik and Fennessy 2016; van de Broek and others 2016; Kelleway and others 2016). Although seagrass meadows can store significant amounts of carbon (Fourqurean and others 2012), the juvenile stocks in the VCR (< 20 years old) contain shallow belowground organic carbon profiles, with organic-rich sediments in the top 3–6 cm that have accumulated since seagrass restoration, far shallower than organic matter depths in salt marshes, which can extend more than a meter deep (Oreska and others 2017; Oreska and others 2017). This results in a smaller spatial carbon density that integrates carbon stored in the top 1 m despite relatively dense carbon in shallow seagrass soils. If seagrasses accumulated soil carbon stores at comparable depths to the other blue carbon systems, the landscape scale carbon storage of seagrass would approximately triple (SI Table 1, Figure 4). Together, we find that positive changes in the carbon stocks of seagrasses did not compensate for the loss of carbon from forests and the other blue

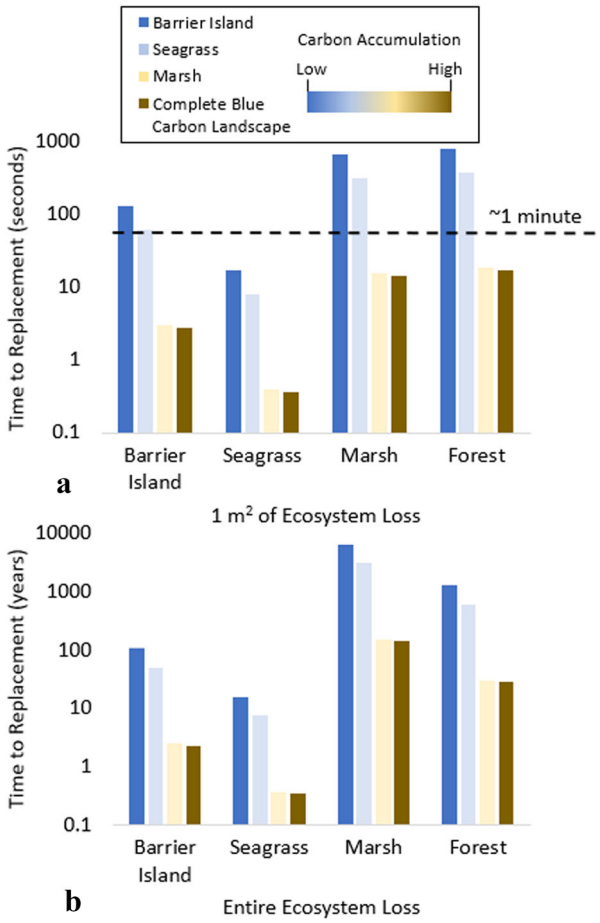

Figure 6. (**a**) The time to replacement (seconds) of carbon lost from the reduction of 1.0 m^2 of the respective ecosystem on the horizontal axis and replaced by the entire carbon accumulating power of the respective ecosystem or landscape in the legend. Ecosystems are plotted along the horizontal axis in order from least to greatest carbon density (g C m^{-2}). This increase in carbon density drives the increase in time to replacement. Meanwhile, the magnitude of carbon accumulation rates, which is smallest in the barrier islands and largest at the coastal landscape scale, decreases time to replacement within a categorical bin. (**b**) The time to replacement (years) of carbon lost from the entire loss of the respective ecosystem across the VCR on the horizontal axis and replaced by the entire carbon accumulating power of the respective ecosystem or landscape in the legend.

carbon habitats, resulting in a landscape-scale reduction in carbon stocks (Figure 5, Table 2). Coastal forests are not typically placed in a blue carbon context, but studies that examine non-wetland coastal forest stocks find similarly high magnitude carbon storage (Smart and others 2020, 2021; Smith and Kirwan 2021; Aguilos and others 2021). The scale of carbon loss observed between 1984 and 2020 (196.9 Gg C) is on a similar scale to other studies that examine the loss of carbon due to overwash, urbanization, or wildfire in other systems (Sirin and others 2020; Zhang and others 2012; Theuerkauf and Rodriguez 2015). While the propagation of dominant landscape features through time mirrors the shifting mosaic steady-state concept, the reduction in regional carbon storage indicates that landscape-scale compensatory functions are temporarily reduced (Figure 4).

Blue carbon ecosystems are well known to be vulnerable to a variety of climate and anthropogenic stressors that threaten the persistence of individual ecosystems and their carbon pools (McLeod and others 2011). However, the broader coastal landscape is uniquely positioned to potentially replace carbon lost from individual points within the landscape because of rapid carbon accumulation rates across a diverse suite of ecosystems. Where ecosystems are lost, high carbon accumulation rates in surviving ecosystems may be able to mediate carbon loss (Figure 5; Elsey-Quirk and others 2011; McLeod and others 2011; Holmquist and others 2018; Smith and Kirwan 2021). For example, despite loss in barrier island volume, the expansion of highly productive shrubs into barrier island grasslands have compensated for carbon loss (Zinnert and others 2016, 2019; Woods and others 2021). Although the time to replacement metric has been largely used to look at the carbon lost and replaced over time at a fixed location (Smith and Kirwan, 2021), the extension of the metric to estimate the time required for an entire landscape to replace lost carbon reveals small landscape scale legacy affects. Specifically, we find that it takes approximately 7 years to replace the 4% reduction in landscape carbon storage observed over 36 years. This metric suggests that surviving ecosystems quickly replace the amount of carbon lost during decadal-scale ecosystem transitions.

The carbon loss for minor reductions in ecosystem extents can be replaced by the entire VCR landscape in a matter of seconds (Figure 6a), but larger scale ecosystem reductions can have a legacy effect on regional carbon storage that last longer than centuries (Figure 6b). As the carbon stock of the lost ecosystem increases, so does the time to replacement and the legacy effect of that carbon loss; carbon lost from 1 m^2 of forest loss takes two orders of magnitude longer to be replaced than carbon lost from 1 m^2 of barrier island (Figure 6a). However, the magnitude of the legacy effect of carbon loss is not only reliant on the magnitude of loss, but also the rate at which it is replaced. Barrier

islands are shown to have the slowest regional soil carbon accumulation rate leading to the slowest compensatory mechanisms in the VCR (Figure 6b).

Similarly, the area over which carbon is replaced can greatly affect the rate of recovery. For example, 1 m^2 of forest loss was estimated to have a legacy effect of 169.6 years when being replaced by 1 m^2 of marsh (Eq. 1; Smith and Kirwan 2021). The legacy effect decreases to $\sim$ 20 s when 1 m^2 of forest loss is replaced by the cumulative area of all the marshes within the VCR (Figure 6a; Eq. 2: 13.9 kg C/25.7 Gg C y^{-1} = 17.7 s). Not only does this indicate that times to replacement will increase with marsh loss, but it also indicates that functional compensation may be scale dependent with weak compensation at local scales and stronger compensation at larger scales. However, as spatial scales increase, so does uncertainty in carbon loss. A global application of the time to replacement metric could reveal compensatory mechanisms across a range of spatial scales, but accounting for changes in carbon storage and accumulation across multiple spatial and temporal scales remains complex.

To project the legacy effect of complete ecosystem loss on the landscape, we apply the time to replacement metric to approximate the amount of time required to replace carbon lost from entire landscape-scale ecosystem collapse (Figure 6b). While this scale of collapse is rare, climate change and urbanization can often result in relatively rapid and irreversible ecosystem loss seen in deforestation and seagrass extirpation (Zhang and others 2012; Arias-Ortiz and others 2018). For example, in the VCR, seagrass became locally extinct due to a combination of hurricane disturbance and an outbreak of seagrass wasting disease in the 1930's (Orth and McGlathery 2012; Orth and others 2020). Within the VCR, if all current seagrass was to experience a similar die-off and the soil carbon stocks were not preserved within the landscape, our analysis indicates that the system would be in a carbon deficit for less than half a year (Figure 6b; Eq. 4: 8.66 Gg C/25.7 Gg C y^{-1} = 0.34 years). Similarly, if forests were suddenly lost, due to wildfire or disease for example, the entire coastal landscape would require approximately 30 years to replace the lost carbon (Figure 6b; Eq. 4: 754 Gg C/25.7 Gg C y^{-1} = 29.3 years). This emphasizes that the coastal landscape is resilient even to rapid, large-scale changes in the carbon dense ecosystems that comprise it.

These time to replacement calculations are based on observed carbon accumulation rates and carbon stocks across a variety of coastal ecosystems, and are therefore inherently simplistic. They do not include dynamic aspects of preservation and decomposition following ecosystem loss, interacting facets of climate change, temporal variability during ecosystem recovery, or couplings and exchanges between ecosystems. Organic matter preservation between systems following ecosystem transition may reduce time to replacement estimates in highly connected landscapes: organic matter produced in marshes contribute to seagrass soil carbon stocks and salt marsh soils can incorporate eelgrass detritus (Greiner and others 2016; Oreska and others 2017; Prentice and others 2020; Ward and others 2021). However, the preservation and connectivity of organic matter between ecosystems in the coastal environment is highly variable. On the other hand, recovering seagrass meadows require a decade for carbon accumulation rates to be equivalent to mature ecosystems (McGlathery and others 2012; Greiner and others 2013), which could substantially increase the time to replacement in seagrass meadows. However, because marshes rather than seagrasses dominate carbon storage and dynamics within this study area, accounting for this lag time in functionality still results in decadal landscape-scale times to replacement. While the refinement of these caveats will improve the accuracy of time to replacement estimates, the rapid replacement of even large-scale carbon reductions implies a functional resilience in the coastal landscape capable of absorbing climate driven reductions in carbon storage.

Accelerating rates of sea level rise are expected to have complex, interacting effects on time to replacement calculations. For example, accelerated sea-level rise has been shown to increase marsh carbon loss through drowning and erosion, but also to increase soil carbon accumulation rates and biomass in surviving marshes (Theuerkauf and Rodriguez 2017; Herbert and others 2021; Chen and Kirwan 2022a; Valentine and others 2023). Beyond marshes, accelerating sea-level rise is expected to affect both current and potential habitable area for seagrasses, but sediment accretion within seagrass meadows can partially offset these losses (Aoki and others 2020). While these biogeomorphic feedbacks have been shown to mitigate functional and spatial reductions in coastal ecosystems, accelerating rates of sea-level rise are projected to exceed critical thresholds potentially leading to widespread ecosystem collapse (Kirwan and Megonigal, 2013). For example, barrier islands exhibit differential responses to sea-level rise, but will likely migrate more rapidly, erode, or drown, resulting in a net carbon loss (Zinnert and others 2019; Mariotti and Hein 2022). Additionally,

coastal squeeze along developed coastlines can undermine compensatory mechanisms and exacerbate net carbon loss (Doody 2013; Pontee 2013; Theuerkauf and Rodriguez 2017) as shown by the diminishing forested land observed in this study (Figure 2). Therefore, while compensatory mechanisms have been shown to quickly compensate for historical losses of carbon, the integrity of these compensatory mechanisms may be expected to diminish as global climate change accelerates. To further examine this, our algebraic time to replacement metrics could be integrated into mechanistic models to respond to coastal dynamics that are expected to change under future higher sea-level rise scenarios.

Conclusions and Implications

Although compensatory mechanisms have traditionally been examined in the context of how populations and communities reorganize following environmental change, our work expands the scope of compensatory mechanism theory to encompass abiotic processes at the scale of entire landforms (that is, spatial and functional compensation). From 1984 to 2020, we found that the landscape composition of a rapidly migrating coastal mosaic remained relatively constant because a majority of landscape losses were compensated by gains elsewhere in the landscape (Table 2, Figure 2). Contrary to this apparent stability, there was a slight reduction in regional carbon storage across the landscape as critical mature ecosystems were unable to spatially compensate losses (Figures 2, 4, 5).

As an immature ecosystem ages, the functionality of the entire system is expected to increase, but accelerating rates in sea-level rise and resulting ecosystem transitions could prevent recovery before net gains in carbon storage are achieved (Smith and Kirwan 2021). In terrestrial forested ecosystems, enhanced woody biomass growth following wildfires can result in functional compensation of lost carbon pools (Kashian and others 2006; Smithwick and others 2009), but only if the system recovers before the next disturbance (Smithwick and others 2009; Brown and Johnstone 2011). In contrast to these findings, the short timescales calculated for the replacement of coastal carbon suggest compensatory mechanisms in the coastal landscape are uniquely suited to maintaining functional rates that exceed ecosystem rates of carbon loss. However, when ecosystems with high carbon accumulation rates are converted to ecosystems with low carbon sequestration, landscape-scale carbon accumulation is reduced. While spatial compensation in this study conserved ecosystem area, rapid loss of area in high carbon accumulating systems, such as the conversion of mangroves to shrimp farms or seagrasses to bare mud, results in decreased regional carbon accumulation, in addition to the initial carbon stock loss (Valiela and others 2001; Aoki and others 2020). Therefore, even if the landscape was able to quickly replace the large magnitude of lost carbon, the reduction of blue carbon ecosystems leads to slower accumulation of long-term carbon stocks in the coastal landscape.

We estimated that it will take less than 8 years for the coastal landscape to compensate for the loss of carbon associated with the landscape changes observed over 36 years (Figure 6). The pace of ecosystem transition and loss of local carbon stocks are fundamentally linked to rates of sea-level rise in barrier islands, marshes, and coastal forests (Theuerkauf and Rodriguez 2017; Smith and Kirwan 2021; Mariotti and Hein 2022), suggesting that accelerating sea-level rise rates will further lengthen the time for carbon pools to recover. Although disturbances associated with climate, storms, and anthropogenic stressors are ubiquitous in coastal landscapes, our estimates of short replacement timescales suggest that functional compensation is possible despite potentially rapid moments of carbon loss. Together with our observations of maintained ecosystem extent, these results suggest that spatial and functional compensation are achieved rapidly at the scale of entire landscapes, and that fast-acting compensatory dynamics may quickly compensate for the carbon lost in rapidly transitioning ecosystems.

Acknowledgements

We would like to acknowledge John Porter for managing the data repository for the VCR LTER from which all field data originated (and can be found in the Supplemental Material). Additionally, we'd like to thank all the graduate students, staff, and volunteers with the VCR LTER involved with the collection of the data collated in the data repository over the past 40+ years. We would also like to thank an anonymous reviewer and the Subject-Matter Editor who provided beneficial comments to improve the manuscript. This work was supported by the National Science Foundation to the University of Virginia for the Virginia Coast Reserve Long-term Ecological Research project (#DEB-1832221). Additional funding was provided by NSF award #1654374, #2012670, #9211772, #9411974, #0080381, #0621014, #1237733.

REFERENCES

Aguilos M, Brown C, Minick K, Fischer M, Ile OJ, Hardesty D, … King, J. 2021. millennial-scale carbon storage in natural pine forests of the North Carolina Lower Coastal Plain: effects of artificial drainage in a time of rapid sea level rise. - Land 10(12):1294.

Aoki LR, McGlathery KJ, Wiberg PL, Al-Haj A. 2020. Depth affects seagrass restoration success and resilience to marine heat wave disturbance. Estuaries and Coasts 43(2):316–328.

Arias-Ortiz A, Serrano O, Masqué P, Lavery PS, Mueller U, Kendrick GA, … Duarte CM. 2018. A marine heatwave drives massive losses from the world's largest seagrass carbon stocks. Nature Climate Change 8(4):338–344.

Benrey B, Denno RF. 1997. The slow-growth–high-mortality hypothesis: a test using the cabbage butterfly. Ecology 78(4):987–999.

Berger AC, Berg P, McGlathery KJ, Delgard ML. 2020. Long-term trends and resilience of seagrass metabolism: A decadal aquatic eddy covariance study. Limnology and Oceanography 65(7):1423–1438.

Bernhardt JR, Leslie HM. 2013. Resilience to climate change in coastal marine ecosystems. Annual Review of Marine Science 5:371–392.

Bormann FH, Likens GE. 2012. *Pattern and process in a forested ecosystem: disturbance, development and the steady state based on the Hubbard Brook ecosystem study*. Springer Science & Business Media.

Brown CD, Johnstone JF. 2011. How does increased fire frequency affect carbon loss from fire? A case study in the northern boreal forest. International Journal of Wildland Fire 20(7):829–837.

Burns CJ, Alexander CR, Alber M. 2021. Assessing long-term trends in lateral salt-marsh shoreline change along a US east coast latitudinal gradient. Journal of Coastal Research 37(2):291–301.

Cai WJ, Hu X, Huang WJ, Jiang LQ, Wang Y, Peng TH, Zhang X. 2010. Alkalinity distribution in the western North Atlantic Ocean margins. Journal of Geophysical Research: Oceans 115(C8).

Chen Y, Kirwan ML. 2022a. Climate-driven decoupling of wetland and upland biomass trends on the mid-Atlantic coast. Nature Geoscience 15(11):913–918.

Chen Y, Kirwan ML. 2022b. A phenology-and trend-based approach for accurate mapping of sea-level driven coastal forest retreat. Remote Sensing of Environment 281:113229.

Deaton CD, Hein CJ, Kirwan ML. 2017. Barrier island migration dominates ecogeomorphic feedbacks and drives salt marsh loss along the Virginia Atlantic Coast, USA. Geology 45(2):123–126.

Doney SC, Ruckelshaus M, Emmett Duffy J, Barry JP, Chan F, English CA, ... Talley LD. 2012. Climate change impacts on marine ecosystems. Annual Review of Marine Science 4:11–37.

Doody JP. 2013. Coastal squeeze and managed realignment in southeast England, does it tell us anything about the future? Ocean & Coastal Management 79:34–41.

Elsey-Quirk T, Seliskar DM, Sommerfield CK, Gallagher JL. 2011. Salt marsh carbon pool distribution in a mid-Atlantic lagoon, USA: sea level rise implications. Wetlands 31(1):87–99.

Ewers Lewis CJ, Baldock JA, Hawke B, Gadd PS, Zawadzki A, Heijnis H, Jacobsen GE, Rogers K, Macreadie PI. 2019. Impacts of land reclamation on tidal marsh 'blue carbon'stocks. Science of the Total Environment 672:427–437.

Fagherazzi S, Mariotti G, Leonardi N, Canestrelli A, Nardin W, Kearney WS. 2020. Salt marsh dynamics in a period of accelerated sea level rise. Journal of Geophysical Research: Earth Surface 125(8):e2019JF005200.

Faunce KE, Rapp JL. 2020. Topobathymetric Digital Elevation Model (TBDEM) of the Eastern Shore Peninsula of Virginia and adjacent parts of Maryland with a horizontal resolution of 1 meter and vertical resolution of 1 centimeter: U.S. Geological Survey data release. https://doi.org/10.5066/P9F5CV1Y.

Fenster MS, Dolan R, Smith JJ. 2016. Grain-size distributions and coastal morphodynamics along the southern Maryland and Virginia barrier islands. Sedimentology 63(4):809–823.

FitzGerald DM, Hughes Z. 2019. Marsh processes and their response to climate change and sea-level rise. Annual Review of Earth and Planetary Sciences 47:481–517.

Flester JA, Blum LK. 2020. Rates of mainland marsh migration into uplands and seaward edge erosion are explained by geomorphic type of salt marsh in Virginia coastal lagoons. Wetlands 40(6):1703–1715.

Folke C, Carpenter S, Walker B, Scheffer M, Elmqvist T, Gunderson L, Holling CS. 2004. Regime shifts, resilience, and biodiversity in ecosystem management. Annu. Rev. Ecol. Evol. Syst. 35:557–581.

Forman RT. 2014. Land Mosaics: The ecology of landscapes and regions (1995). *The ecological design and planning reader*, 217–234.

Fourqurean JW, Duarte CM, Kennedy H, Marbà N, Holmer M, Mateo MA, Apostolaki ET, Kendrick GA, Krause-Jensen D, McGlathery KJ, Serrano O. 2012. Seagrass ecosystems as a globally significant carbon stock. Nature Geoscience 5(7):505–509.

Fryer J, Williams ID. 2021. Regional carbon stock assessment and the potential effects of land cover change. Science of the Total Environment 775:145815.

Gamache I, Payette S. 2005. Latitudinal response of subarctic tree lines to recent climate change in eastern Canada. Journal of Biogeography 32(5):849–862.

Garrard SL, Beaumont NJ. 2014. The effect of ocean acidification on carbon storage and sequestration in seagrass beds; a global and UK context. Marine Pollution Bulletin 86(1–2):138–146.

Ghedini G, Russell BD, Connell SD. 2015. Trophic compensation reinforces resistance: herbivory absorbs the increasing effects of multiple disturbances. Ecology Letters 18(2):182–187.

Greiner JT, McGlathery KJ, Gunnell J, McKee BA. 2013. Seagrass restoration enhances ''blue carbon'' sequestration in coastal waters. PloS One 8(8):e72469.

Greiner JT, Wilkinson GM, McGlathery KJ, Emery KA. 2016. Sources of sediment carbon sequestered in restored seagrass meadows. Marine Ecology Progress Series 551:95–105.

Guimond JA, Yu X, Seyfferth AL, Michael HA. 2020. Using hydrological-biogeochemical linkages to elucidate carbon dynamics in coastal marshes subject to relative sea level rise. Water Resources Research, 56(2):e2019WR026302.

Hartig EK, Gornitz V, Kolker A, Mushacke F, Fallon D. 2002. Anthropogenic and climate-change impacts on salt marshes of Jamaica Bay, New York City. Wetlands 22(1):71–89.

Hayden BP, Dueser RD, Callahan JT, Shugart HH. 1991. Long-term research at the Virginia Coast Reserve. BioScience 41(5):310–318.

He C, Zhang D, Huang Q, Zhao Y. 2016. Assessing the potential impacts of urban expansion on regional carbon storage by linking the LUSD-urban and InVEST models. Environmental Modelling & Software 75:44–58.

Herbert ER, Windham-Myers L, Kirwan ML. 2021. Sea-level rise enhances carbon accumulation in United States tidal wetlands. One Earth 4(3):425–433.

Holmquist JR, Windham-Myers L, Bliss N, Crooks S, Morris JT, Megonigal JP, ... Woodrey, M. 2018. Accuracy and precision of tidal wetland soil carbon mapping in the conterminous United States. Scientific Reports 8(1):1–16.

Houlahan JE, Currie DJ, Cottenie K, Cumming GS, Ernest SKM, Findlay CS, ... Wondzell SM. 2007. Compensatory dynamics are rare in natural ecological communities. Proceedings of the National Academy of Sciences 104(9):3273–3277.

Kashian DM, Romme WH, Tinker DB, Turner MG, Ryan MG. 2006. Carbon storage on landscapes with stand-replacing fires. Bioscience 56(7):598–606.

Kelleway JJ, Saintilan N, Macreadie PI, Ralph PJ. 2016. Sedimentary factors are key predictors of carbon storage in SE Australian saltmarshes. Ecosystems 19(5):865–880.

Kirwan ML, Gedan KB. 2019. Sea-level driven land conversion and the formation of ghost forests. Nature Climate Change 9(6):450–457.

Kirwan ML, Megonigal JP. 2013. Tidal wetland stability in the face of human impacts and sea-level rise. Nature 504(7478):53–60.

Loreau M, De Mazancourt C. 2013. Biodiversity and ecosystem stability: a synthesis of underlying mechanisms. Ecology Letters 16:106–115.

MacArthur RH, Diamond JM, Karr JR. 1972. Density compensation in island faunas. Ecology 53(2):330–342.

Macreadie PI, Nielsen DA, Kelleway JJ, Atwood TB, Seymour JR, Petrou K, ... Ralph PJ. 2017. Can we manage coastal ecosystems to sequester more blue carbon?. Frontiers in Ecology and the Environment 15(4):206–213.

Maher EL, Germino MJ, Hasselquist NJ. 2005. Interactive effects of tree and herb cover on survivorship, physiology, and microclimate of conifer seedlings at the alpine tree-line ecotone. Canadian Journal of Forest Research 35(3):567–574.

Mariotti G, Hein CJ. 2022. Lag in response of coastal barrier-island retreat to sea-level rise. Nature Geoscience 15(8):633–638.

May SK, Dolan R, Hayden BP. 1983. Erosion of US shorelines. Eos, Transactions American Geophysical Union 64(35):521–523.

Mcleod E, Chmura GL, Bouillon S, Salm R, Björk M, Duarte CM, ... Silliman BR. 2011. A blueprint for blue carbon: toward an improved understanding of the role of vegetated coastal habitats in sequestering CO2. Frontiers in Ecology and the Environment 9(10):552–560.

McGlathery KJ, D'Odorico P, Fagherazzi S, Pace M, Reidenbach M. 2013. Nonlinear dynamics and alternate stable states in shallow coastal systems. Oceanography 26(3):220–231. https://doi.org/10.5670/oceanog.2013.66.

McGlathery KJ, Reynolds LK, Cole LW, Orth RJ, Marion SR, Schwarzschild A. 2012. Recovery trajectories during state change from bare sediment to eelgrass dominance. Marine Ecology Progress Series 448:209–221.

McLoughlin SM, Wiberg PL, Safak I, McGlathery KJ. 2015. Rates and forcing of marsh edge erosion in a shallow coastal bay. Estuaries and Coasts 38:620–638.

Molino GD, Defne Z, Aretxabaleta AL, Ganju NK, Carr JA. 2021. Quantifying slopes as a driver of forest to marsh conversion using geospatial techniques: application to chesapeake bay coastal-plain. United States. Frontiers in Environmental Science 9:149.

Morton RA. 2008. *National assessment of shoreline change: Part 1: Historical shoreline changes and associated coastal land loss along the US Gulf of Mexico*. Diane Publishing.

Nahlik AM, Fennessy M. 2016. Carbon storage in US wetlands. Nature Communications 7(1):1–9.

Oreska MP, McGlathery KJ, Porter JH. 2017. Seagrass blue carbon spatial patterns at the meadow-scale. PloS One 12(4):e0176630.

Orr JC, Epitalon JM, Gattuso JP. 2015. Comparison of ten packages that compute ocean carbonate chemistry. Biogeosciences 12(5):1483–1510.

Orr JC, Epitalon JM, Dickson AG, Gattuso JP. 2018. Routine uncertainty propagation for the marine carbon dioxide system. Marine Chemistry 207:84–107.

Orth RJ, Lefcheck JS, McGlathery KS, Aoki L, Luckenbach MW, Moore KA, Oreska MP, Snyder R, Wilcox DJ, Lusk B. 2020. Restoration of seagrass habitat leads to rapid recovery of coastal ecosystem services. Science Advances 6(41):eabc6434.

Orth RJ, McGlathery KJ. 2012. Eelgrass recovery in the coastal bays of the Virginia Coast Reserve, USA. Marine Ecology Progress Series 448:173–176.

Pontee N. 2013. Defining coastal squeeze: A discussion. Ocean & Coastal Management 84:204–207.

Prentice C, Poppe KL, Lutz M, Murray E, Stephens TA, Spooner A, Hessing-Lewis M, Sanders-Smith R, Rybczyk JM, Apple J, Short FT. 2020. A synthesis of blue carbon stocks, sources, and accumulation rates in eelgrass (Zostera marina) meadows in the Northeast Pacific. Global Biogeochemical Cycles 34(2):e2019GB006345.

Safak I, Wiberg PL, Richardson DL, Kurum MO. 2015. Controls on residence time and exchange in a system of shallow coastal bays. Continental Shelf Research 97:7–20.

Sallenger AH, Doran KS, Howd PA. 2012. Hotspot of accelerated sea-level rise on the Atlantic coast of North America. Nature Climate Change 2(12):884–888.

Schieder NW, Walters DC, Kirwan ML. 2018. Massive upland to wetland conversion compensated for historical marsh loss in Chesapeake Bay, USA. Estuaries and Coasts 41(4):940–951.

Siikamäki J, Sanchirico JN, Jardine S, McLaughlin D, Morris D. 2013. Blue carbon: coastal ecosystems, their carbon storage, and potential for reducing emissions. Environment: Science and Policy for Sustainable Development 55(6):14–29.

Sirin AA, Makarov DA, Gummert I, Maslov AA, Gul'be YI. 2020. Depth of peat burning and carbon loss during an underground forest fire. Contemporary Problems of Ecology 13(7):769–779.

Smart LS, Taillie PJ, Poulter B, Vukomanovic J, Singh KK, Swenson JJ, ... Meentemeyer RK. 2020. Aboveground carbon loss associated with the spread of ghost forests as sea levels rise. Environmental Research Letters 15(10):104028.

Smart LS, Vukomanovic J, Taillie PJ, Singh KK, Smith JW. 2021. Quantifying Drivers of Coastal Forest Carbon Decline Highlights Opportunities for Targeted Human Interventions. Land 10(7):752.

Smith AJ, Kirwan ML. 2021. Sea Level-Driven Marsh Migration Results in Rapid Net Loss of Carbon. Geophysical Research Letters 48(13):e2021GL092420.

Smith AJ, Noyce GL, Megonigal JP, Guntenspergen GR, Kirwan ML. 2022. Temperature optimum for marsh resilience and carbon accumulation revealed in a whole-ecosystem warming experiment. Global Change Biology.

Smithwick EAH, Ryan MG, Kashian DM, Romme WH, Tinker DB, Turner MG. 2009. Modeling the effects of fire and climate change on carbon and nitrogen storage in lodgepole pine (Pinus contorta) stands. Global Change Biology 15(3):535–548.

Theuerkauf EJ, Rodriguez AB. 2017. Placing barrier-island transgression in a blue-carbon context. Earth's Future 5(7):789–810.

Torio DD, Chmura GL. 2013. Assessing coastal squeeze of tidal wetlands. Journal of Coastal Research 29(5):1049–1061.

Trevathan-Tackett SM, Wessel C, Cebrián J, Ralph PJ, Masqué P, Macreadie PI. 2018. Effects of small-scale, shading-induced seagrass loss on blue carbon storage: Implications for management of degraded seagrass ecosystems. Journal of Applied Ecology 55(3):1351–1359.

Turner MG. 2010. Disturbance and landscape dynamics in a changing world. Ecology 91(10):2833–2849.

Van de Broek M, Temmerman S, Merckx R, Govers G. 2016. Controls on soil organic carbon stocks in tidal marshes along an estuarine salinity gradient. Biogeosciences 13(24):6611–6624.

Van Heuven SMAC, Pierrot D, Rae JWB, Lewis E, Wallace DWR. 2011. MATLAB program developed for CO2 system calculations. ORNL/CDIAC-105b:530.

Valentine K, Herbert ER, Walters DC, Chen Y, Smith AJ, Kirwan ML. 2023. Climate-driven tradeoffs between landscape connectivity and the maintenance of the coastal carbon sink. Nature Communications 14(1):1137.

Valiela I, Bowen JL, York JK. 2001. Mangrove forests: one of the world's threatened major tropical environments: at least 35% of the area of mangrove forests has been lost in the past two decades, losses that exceed those for tropical rain forests and coral reefs, two other well-known threatened environments. Bioscience 51(10):807–815.

Ward MA, Hill TM, Souza C, Filipczyk T, Ricart AM, Merolla S, Capece LR, O'Donnell BC, Elsmore K, Oechel WC, Beheshti KM. 2021. Blue carbon stocks and exchanges along the California coast. Biogeosciences 18(16):4717–4732.

Woods NN, Tuley PA, Zinnert JC. 2021. Long-term community dynamics reveal different trajectories on two mid-Atlantic coast maritime forests. Forests 12:1063.

Zhang C, Tian H, Chen G, Chappelka A, Xu X, Ren W, ... Lockaby G. 2012. Impacts of urbanization on carbon balance in terrestrial ecosystems of the Southern United States. Environmental Pollution 164:89–101.

Zinnert JC, Via SM, Nettleton BP, Tuley PA, Moore LJ, Stallins JA. 2019. Connectivity in coastal systems: barrier island vegetation influences upland migration in a changing climate. Global Change Biology 25:2419–2430.

Zinnert JC, Shiflett SA, Via SM, Bissett SN, Dows B, Manley P, Young DR. 2016. Spatio-temporal dynamics in barrier island upland vegetation: the overlooked coastal landscape. Ecosystems 19:685–697.